Polymer Testing 40 (2014) 99–105

Contents lists available at ScienceDirect

Polymer Testing

journal homepage: www.elsevier.com/locate/polytest

Material properties

Influence of cellulose nanofibrils on soft and hard segments of polyurethane/cellulose nanocomposites and effect of humidity on their mechanical properties

Alex Otávio Sanches [a], Luciano Henrique Siliano Ricco [a], Luiz Francisco Malmonge [a], Michael Jones da Silva [b], Walter Katsumi Sakamoto [a], José Antonio Malmonge [a, *]

[a] Departamento de Física e Química, Faculdade de Engenharia, UNESP – Univ. Estadual Paulista, Campus de Ilha Solteira, Ilha Solteira, SP, Brazil
[b] UNESP – Univ. Estadual Paulista, Campus Experimental de Rosana, Rosana, SP, Brazil

ARTICLE INFO

Article history:
Received 3 July 2014
Accepted 12 August 2014
Available online 4 September 2014

Keywords:
Particle-reinforcement
Cellulose nanofibrils
Nanocomposite
Polyurethane

ABSTRACT

Cellulose nanofibrils (CNFs) were prepared by sulfuric acid hydrolysis from cotton microfibers, and used to prepare polyurethane (PU) nanocomposites by mixing CNF_S and PU water suspensions. CNFs as nanofillers improved the tensile strength of PU significantly up to 10 wt% content. With an increase in the CNF content, the glass transition temperature of PU and the temperature onset of the soft segment increased compared with those of neat PU. However, the crystalline phase present in soft domains and its melting temperature decreased. The influences of humidity on the mechanical properties of PU/CNF nanacomposites were also investigated. The tensile strength at different elongations of PU/CNF nanocomposites decreased substantially after being exposed to 60% relative humidity for 24 h; for 10 wt% loading, the tensile strength at 500% dropped from 10.64 to 2.34 MPa. This behavior was attributed to the formation of hydrogen bonds of PU and CNFs with water.

1. Introduction

The introduction of nanoparticles into polymer matrices has attracted considerable attention because it can significantly improve the thermal and mechanical properties of the polymeric matrix even at very low contents [1–5]. Among the nanofillers used as reinforcements, cellulose nanofibers have been highlighted owing to their biodegradability, low density, high aspect ratio, easy availability and low cost [1,2,6–38]. Cellulose is a polysaccharide consisting of linear chains composed of β-D-glucopyranose repeating units linked by (1–4)-glycosidic bonds. Cellulose microfibers consist of ordered regions, commonly referred to as nanofibrils, nanowhiskers or whiskers, linked by amorphous cellulose chains. These nanofibrils can be extracted by controlled acid hydrolysis, which more readily hydrolyses the amorphous regions, leaving crystals with diameters and lengths that directly depend on the hydrolysis conditions and source [21]. When strong sulfuric acid is used, negatively charged sulfate groups are introduced and, consequently, stable aqueous suspensions are obtained. Cellulose nanofibers have abundant hydroxyl groups (OH) on the surface that can form hydrogen bonds with the polymer matrix and between nanofibers, developing a strong reinforcement. Cellulose nanofibers have been incorporated as reinforcing fillers in a wide range of polymer matrixes such as poly(β-hydroxyoctanoate) [7], poly(styrene-

* Corresponding author. Tel.: +55 (18) 37431029.
E-mail addresses: mal@dfq.feis.unesp.br, jamalmonge@yahoo.com.br (J.A. Malmonge).

http://dx.doi.org/10.1016/j.polymertesting.2014.08.013
0142-9418/

co-butyl acrylate) [8], poly(vinyl chloride) [9], polypropylene [10], waterborne epoxy [11], poly(vinyl alcohol) [12], poly(-acrylic acid) [13], polyethylene oxide [14], poly(lactic acid) [15], polystyrene [16], polymethylmethacrylate [17] and rubbers [18-19], including polyurethane.

Segmented thermoplastic polyurethanes are very versatile polymers that are typically constructed by alternating soft (SS) and hard (HS) segments that are separated into microphases owing to thermodynamic incompatibility between the segments. Generally, HS can be organized in semi-crystalline or amorphous domains, whereas SS form an amorphous or elastic region in which the HS are dispersed [32]. The ratio between SS and HS present in the polyurethane chain can be easily manipulated to give a wide range of polyurethanes with various properties and applications [31–34].

This study reports the preparation and characterization of nanocomposites of water-based polyurethane with cellulose nanofibrils. The nanofibrils were extracted by acid hydrolysis from cotton microfibrils and introduced into a waterborne polyurethane elastomer to prepare PU/CNF nanocomposites with different loading levels of CNF. The present study focuses on the favored interaction of cellulose nanofibrils with SS and HS of polyurethane, as well as the behavior of the reinforcing properties of nanofibers against humidity. This study shows that although the nanofibrils strongly mechanically reinforce the polyurethane, they largely lose their reinforcing properties when subjected to humidity, even at fractions above the percolation threshold.

2. Materials and methods

2.1. Materials

Cotton fibers with a particle size of 50 μm (Sigmacell Cellulose type 50) were purchased from Sigma-Aldrich. Nanofibrils were dialyzed in Spectra/Por Dialysis Membranes with the following characteristics: membrane tube type RC, MWCO: 12 to 14.000, 75-mm flat width, vol/length = 18 mL/cm, length = 15 mm. Concentrated sulfuric acid (98%) was purchased from Sigma-Aldrich and used as received. Waterborne polyurethane with trade name Witicobond W-320 was kindly supplied by Chemtura Corporation.

2.2. Extraction of cellulose nanofibrils

A colloidal suspension of CNFs in water was extracted by acid hydrolysis according to the procedure described by Dong et al. [37]. Cotton microcrystalline cellulose microfibers (MCC) were immersed in a sulfuric acid solution (64% w/v) at 45°C using a MCC:acid solution ratio of 1:7.1 g/mL. The mixture was stirred vigorously for 90 min and then diluted 5-fold with cold deionized water (5°C) to quench the reaction. The resulting dispersion was centrifuged at 10,000 rpm for 10 min at 10°C to separate nanofibrils from the acidic solution. The sediment containing the nanocrystals was dispersed in water and centrifuged again. This operation was performed three times, and the final sediment was dispersed in 150 mL deionized water, followed by dialysis against water until its pH became ~5.

2.3. Nanocomposite preparation

PU/CNF nanocomposites were obtained by mixing the CNF dispersion with PU water suspension in the desired amount. The mixtures were magnetically stirred for 4 h and then cast onto glass slides (75 × 25 × 1.2 mm), which were allowed to dry in a conventional oven at 60°C for 3 h. A series of nanocomposite films containing 5, 10, 15, and 20 wt% of CNFs with a thickness of 0.3–0.4 mm were prepared and designated as PU_5% CNF, PU_10% CNF, PU_15% CNF, and PU_20% CNF, respectively.

2.4. Characterization

The CNF morphology was characterized by a Supra 35 Zeiss field-emission scanning electron microscope (FESEM). 5 μL of CNF aqueous suspension (4.3 g/100 mL) was diluted in 1 mL of isopropyl alcohol, and 3 μL of the resultant suspension was cast onto silicon substrates, dried in dynamic vacuum for 1 h at room temperature and coated with carbon by sputtering prior to FESEM analysis. The morphology of the cryogenically fractured surfaces of PU/CNF nanocomposites was analyzed using an EVO LS15 Zeiss scanning electron microscope (SEM). The test samples were attached to an aluminum stub and sputtered with gold prior to analysis. XRD patterns of the films were obtained by using a Shimadzu XDR-6000 diffractometer with Cu Kα radiation (wavelength: ~1.5418 Å). Scans were carried out from $2\Theta = 5^\circ$ to 60° at a scan rate of 1°/min. DSC analysis of the film scans was performed using a TA Instruments MDSC 2920 calorimeter. Two temperature and heating rate ranges were used to evaluate the thermal behavior of the composites and pure polymer. In the first run, the samples were scanned from −20 to 200°C at 10°C/min to verify the melting temperature (T_m) and enthalpy (ΔH). In the second run, to verify the glass transition temperature (T_g), the samples were scanned from −100 to 150°C at 20°C/min. In both cases, the measurement was conducted in nitrogen atmosphere with a flux flow rate of 65 mL/min. TGA of the films was conducted in the temperature range 25–680°C at a heating rate of 10°C/min in nitrogen atmosphere with a flow rate of 100 mL/min using a TA Instruments model Q600. The mechanical behavior of the nanocomposites was studied at room temperature using an Instron model 3639 universal testing machine in according with ISO 37:2011 using a load cell of 100 N and crosshead speed of 13 mm/min. The samples were cut according to ISO 1286:2006, and the results were averaged from five test specimen data. To analyze the influence of absorbed water on the mechanical properties of the nanocomposites, the samples were keep in dynamic vacuum for 24 h, weighed and then left for 24 h in a chamber with humidity controlled at 30% or 60% relative humidity. Then, the samples were weighed again and immediately subjected to a tensile test. The absorbed water (*WA*) was calculated using the following equation:

$$\mathrm{WA}\ (\%) = \left(\frac{W_t - W_0}{W_0}\right) \times 100 \qquad (1)$$

where W_0 is the sample mass after vacuum and W_t, that after humidity exposure.

3. Results and discussion

3.1. Morphology of CNF_S

Fig. 1 presents the FESEM micrograph of the hydrolyzed cellulose. The resulting structure showed a rod-like shape having nanoscale dimensions with a rod-like shape with an average diameter and length of $D = 31 \pm 11$ nm and $L = 361 \pm 129$ nm. Therefore, the average aspect ratio (L/D) of the CNFs was ~12. These values are in agreement with those reported by others in literature for CNFs extracted from cotton fiber [21,38].

3.2. Morphology of PU/CNFs nanocomposites

Fig. 2 shows images of cryofractured surfaces of the PU/CNF nanocomposites and neat PU. A large contrast can be observed between the fractured surfaces. The composite surface exhibits greater roughness compared to neat PU, indicating an increase in energy dissipation during fracture owing to the presence of nanofibrils. The CNFs were identified as small white dots on the fracture surfaces, and good dispersion of CNF can be observed in the matrix mainly with low concentration. Good dispersion is attributed to the hydrogen bond between the cellulose hydroxyl group and the urethane groups.

3.3. Thermal analysis

Fig. 3a shows the DSC curves of the PU/CNF nanocomposites with various CNF loading levels as well as neat PU. A single glass transition temperature T_g was observed for neat PU; this temperature increased with the amount of CNFs. T_g varied from −14.9°C to −10.4°C for neat PU and PU_20% CNF, respectively, as shown in Fig. 3b. The addition of CNFs hampers SS to move owing to nitrogen bonds between the CNF surface and SS. The endothermic temperature peak was around 44.9°C for neat PU, and was attributed to the melting of the crystalline phase present in the soft domains, with the shift toward low temperature with increasing CNF content indicating a decrease in the crystallite size. Furthermore, the enthalpy of fusion decreases with an increase in nanofibrils loading, demonstrating that the degree of crystallinity of the composite materials also decreases (Fig. 3b). These results are similar to those reported by Saralegy et al. [34] for high cellulose concentration.

Fig. 4a shows the TG/DTG curves of neat PU, CNF, and PU/CNF nanocomposites having various CNF loading levels. The polyurethane TGA profile basically shows three ranges of weight loss. The first, below 100°C, is attributed to water evaporation. The second, from 339°C to 365°C, is attributed to HS decomposition. The last one, from 386°C to 401°C, is attributed to the thermal decomposition of SS. The thermogram of CNF showed the typical degradation profile of CNF hydrolyzed with sulfuric acid. The intense peak at 186°C is attributed to cellulose depolymerization and the dehydration and decomposition of glycosyl units [1] arising from the outermost crystalline regions being subjected to the catalytic effect of sulfate groups. The small shoulder at 257°C can be attributed to the breakage of the crystalline fraction of nanocrystals that was not attacked by the acid [36,39]. The peak at 370°C can be attributed to the oxidation and breakdown of the char to lower-molecular-weight gaseous products [39]. The broad peak centered ~67°C was attributed to the loss of mass owing to the evaporation of water. The TGA profile of nanocomposite samples showed three ranges of weight loss. The first, below 90°C, was attributed to water evaporation, and the other two were associated with HS (339–365°C) and SS (386–401°C) PU degradation. Interestingly, the polyurethane SS possessed higher heat resistance in the composite than neat PU, as

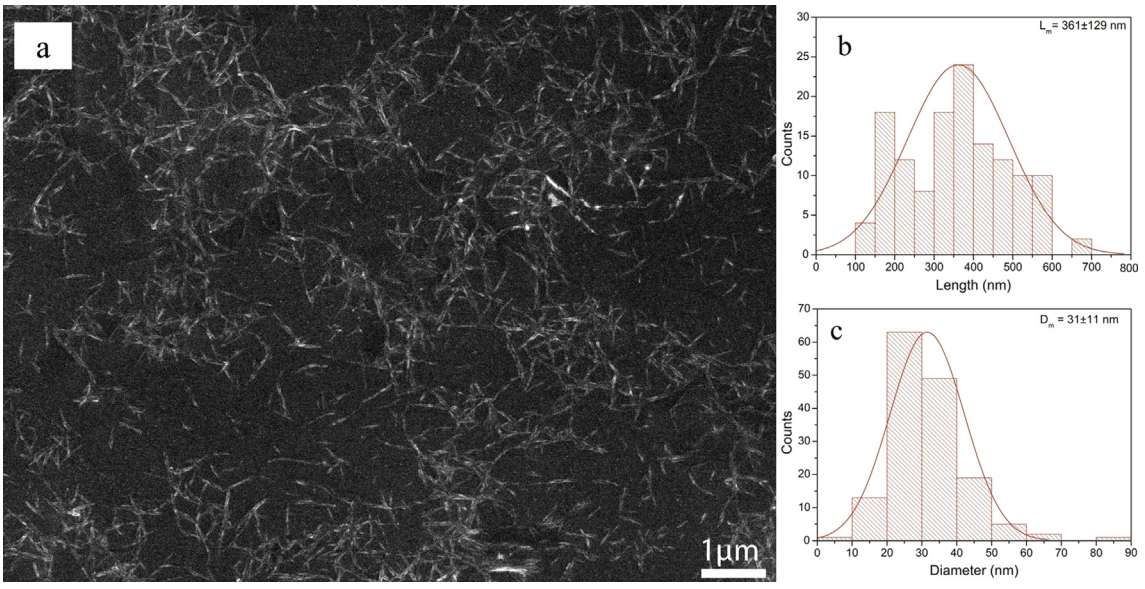

Fig. 1. (a) FESEM image of CNFs and its size statistics for (b) length and (c) diameter. The dashed line represents the Gaussian distribution fitting line according to the statistical data.

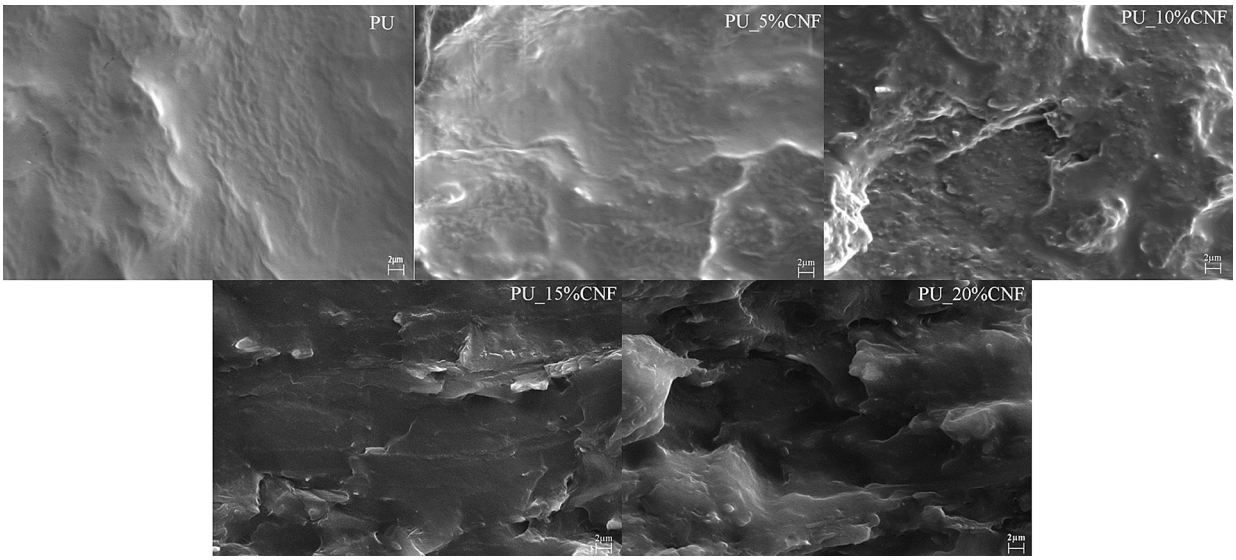

Fig. 2. SEM images of cryofractured surfaces of the PU and PU/CNF composites with different CNF contents: 5, 10, 15, and 20 wt%.

shown in Fig. 4b. On the contrary, the HS's resistance to thermal degradation decreases with an increase in the CNF content in the matrix. This was attributed to the fostering interaction between the CNF and SS of polyurethane and the resulting decrease in the original interaction between SS and HS. These results were also consistent with those obtained from the DSC measurements.

Fig. 5 shows XRD patterns of CNF, PU, and PU/CNF nanocomposites. Three peaks at $2\theta = 15^{\circ}$ (d = 5.9 Å), 16.5° (d = 5.3 Å), 22.6° (d = 3.9 Å), and 34.5° (d = 2.6 Å) were observed for CNF; these are typical of crystalline cellulose type I [27]. Neat PU shows two diffraction peaks at $2\theta = 19.32^{\circ}$ and 23.50°, whereas the PU-heat treated at 50°C for 15 min showed no such peaks. This behavior indicates that these peaks are characteristics of the crystalline PU soft phase. Increasing the CNF content in PU reduced the crystallinity, as confirmed by the enthalpy measurement. The cellulose peaks became more evident in the nanocomposites as the CNF content increased, as expected.

3.4. Mechanical properties

Fig. 6a shows the stress-strain curves of PU and PU/CNF nanocomposites. Neat PU shows the typical behavior of an elastomeric material, exhibiting high flexibility and deformation. The addition of CNF substantially impacted the mechanical properties of the nanocomposites, as shown in Fig. 6b. The highest value of tensile strength was obtained at 500% deformation for a composite loaded with 10 wt% of nanofibrils, increasing from 6.5 MPa for neat PU to 10.5 MPa, an increase of ~61%. It was observed that for CNF content over 10 wt%, the tensile stress at 100% and 300% deformation tends to be constant. This behavior can be attributed to CNF self-agglomeration and percolation processes that can be estimated using the following equation [21]:

$$V_{RC} = \frac{0,7}{(L/D)} \tag{2}$$

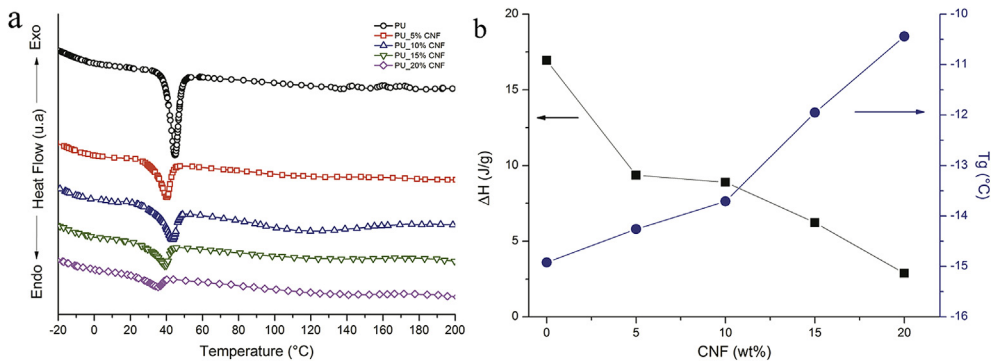

Fig. 3. (a) DSC curves (b) Tg and enthalpy of neat PU and PU/CNF composites with different CNF loadings.

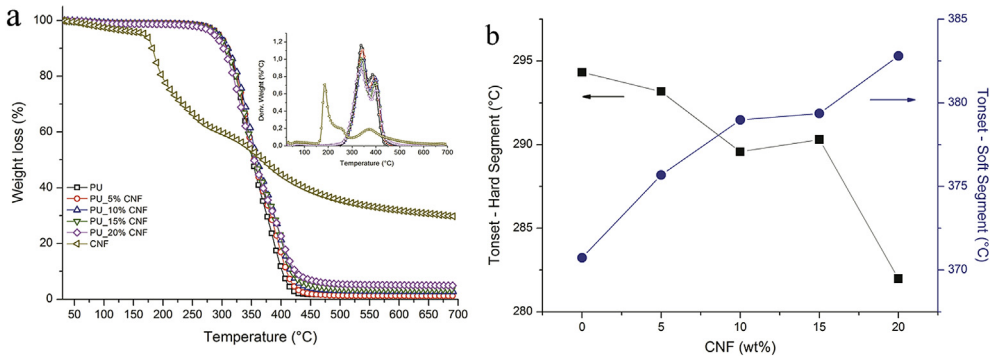

Fig. 4. (a) TG and. (b) Temperature onset of SS and HS of PU with different CNF loadings. Inset: DTG curves of CNF, PU, and PU/CNF composites.

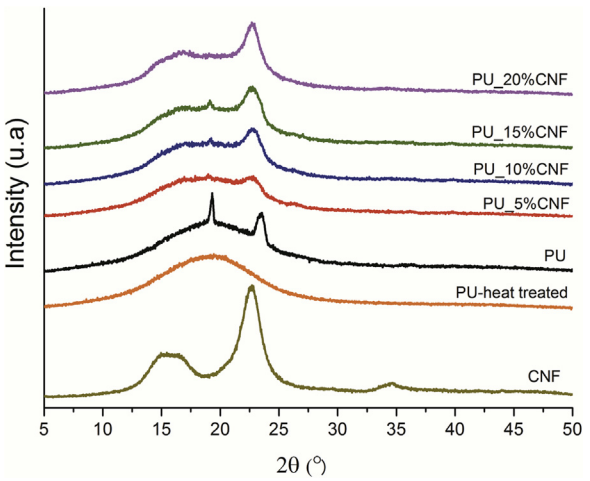

Fig. 5. XRD pattern of CNF, PU, PU heat-treated at 50°C, and PU/CNF composites with different CNF loadings.

where L and D are the average length and diameter of nanofibrils, respectively. In this manner, a percolation threshold of ~5.6 vol% or 8 wt% is obtained using the density values of 1.5 and 1.04 g/cm^3 for CNC and polyurethane, respectively.

Several studies have shown that the introduction of cellulose whiskers significantly reinforces a number of polymers owing to the formation of a three-dimensional hydrogen-bonded CNF network within the polymer matrices [1–2,18–21,34,36]. This interaction can be strongly affected by exposure of the material to water. In some cases, water uptake can be governed by the polymer matrix; in others, it is transported through the cellulose nanofibril network. We investigated the influence of water uptake on the mechanical properties of the nanocomposites; Table 1 summarizes the obtained results. All the nanocomposites and neat PU did not show a change in mass when exposed to 30% relative humidity. However, at 60%, a small amount of absorbed water was observed, and this amount increased with the CNF content in the matrix, indicating that water uptake was controlled by both PU and CNF.

The mechanical properties showed a significant change when the samples were exposed to 60% relative humidity for 24 h, as shown in Table 1. The tensile stress at 100%, 300%, and 500% deformation decreased significantly. The tensile strength of neat PU at break decreased from 10.17 to 2.24 MPa, and the deformation increased from 654% to 1076%. A slight increase in tensile stress at 100%, 300%, and 500% deformation was observed with an increase in CNF loading until 15 wt%. It is well known that the hydrogen

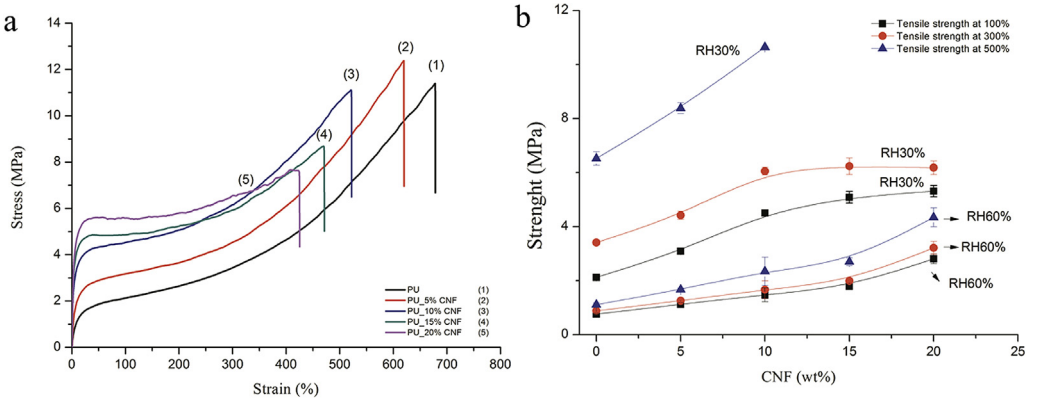

Fig. 6. (a) Representative stress-strain curves for (1) PU, (2) PU_5% CNF, (3) PU_10% CNF, (4) PU_15% CNF, and (5) PU_20% CNF, and (b) tensile strength at 100%, 300%, and 500% elongation of neat PU and PU/CNF nanocomposites with different CNF loading levels.

Table 1
Values of the water absorption (WA); tensile strength at 100% ($\sigma_{100\%}$), 300% ($\sigma_{300\%}$), and 500% ($\sigma_{500\%}$) deformation; tensile strength at break ($\sigma_{at\ break}$); and elongation at break ($\varepsilon_{at\ break}$) of neat PU and PU/CNF nanocomposites exposed to 30% and 60% relative humidity (RH) for 24 h.

Sample	WA (%)	$\sigma_{100\%}$ (MPa)	$\sigma_{300\%}$ (MPa)	$\sigma_{500\%}$ (MPa)	$\sigma_{at\ break}$ (MPa)	$\varepsilon_{at\ break}$ (%)
30% Relative Humidity						
PU	–	2.12 ± 0.03	3.41 ± 0.09	6.52 ± 0.25	10.17 ± 1.61	654.78 ± 38.26
PU_5% CNF	–	3.09 ± 0.10	4.42 ± 0.15	8.38 ± 0.20	11.61 ± 1.43	607.88 ± 22.77
PU_10% CNF	–	4.5 ± 0.10	6.05 ± 0.15	10.64 ± 0.03	10.23 ± 0.72	505.76 ± 17.53
PU_15% CNF	–	5.08 ± 0.22	6.23 ± 0.30	–	8.79 ± 0.69	472.35 ± 19.06
PU_20% CNF	–	5.31 ± 0.21	6.18 ± 0.25	–	7.08 ± 0.61	404.30 ± 39.19
60% Relative Humidity						
PU	1.51 ± 0.15	0.76 ± 0.02	0.88 ± 0.03	1.11 ± 0.07	2.24 ± 0.19	1076.52 ± 71.26
PU_5% CNF	1.74 ± 0.26	1.12 ± 0.05	1.25 ± 0.03	1.67 ± 0.05	3.66 ± 0.23	982.67 ± 33.45
PU_10% CNF	1.84 ± 0.17	1.47 ± 0.26	1.66 ± 0.33	2.34 ± 0.52	3.31 ± 0.76	691.53 ± 51.57
PU_15% CNF	2.03 ± 0.24	1.78 ± 0.10	1.99 ± 0.11	2.70 ± 0.14	3.25 ± 0.35	644.51 ± 39.90
PU_20% CNF	2.21 ± 0.25	2.81 ± 0.18	3.21 ± 0.23	4.34 ± 0.35	4.55 ± 0.25	538.64 ± 35.66

bond is an important physical interaction in waterborne polyurethane that affects the microphase separation structure and mechanical properties [40]. The hydrogen bond can be formed by the hydrogen atom of the urethane group of HS with −C=O and of SS with −C=O. With the introduction of CNF in the PU matrix, hydrogen bonds are formed between the matrix-CNF and CNF-CNF. Under higher relative humidity conditions, the films showed water uptake, and some hydrogen bonds between the polyurethane segments, polyurethane segments-CNF, and CNF-CNF were broken, and others constituted with water. This produced a plasticizing effect that led to a decrease in tensile strength and increase in elongation. In this case, the reinforcement properties of CNFs were drastically reduced, even above the percolation threshold.

4. Conclusions

Cellulose nanofibrils were prepared by sulfuric acid hydrolysis from cotton microfibers and used as nanofillers to improve the properties of PU. SEM showed that CNFs were dispersed homogenously within the PU matrix up to 10 wt%. Increasing the CNF content in PU promoted an increase in T_g and T_{onset} of SS, and a decrease in the crystalline phase present in soft domains as well as its melting temperature. The addition of CNF up to 10 wt% content substantially impacted the mechanical properties of the nanocomposites, reaching a tensile strength of 10.5 MPa at 500% deformation, which is ~61% higher than that of pure PU. The tensile stress at different deformations decreased significantly by increasing the humidity. Water uptake, which leads to the formation of hydrogen bonds with the CNF surface and with PU segments, may explain the changes in the mechanical properties of PU and nanocomposites.

Acknowledgements

The authors acknowledge the Brazilian agencies FAPESP (Process: 12/23637-1) and CNPq (Process: 306753/2012-0) for their financial support.

References

[1] C. Xiaodong, H. Youssef, A.L. Lucian, One-pot polymerization, surface grafting, and processing of waterborne polyurethane-cellulose nanocrystal nanocomposites, J. Mater. Chem. 19 (1) (2009) 7137–7145.
[2] E. Abraham, B. Deepa, L.A. Pothan, M. John, S.S. Narine, S. Thomas, et al., Physicomechanical properties of nanocomposites based on celulose nanofiber and natural rubber latex, Cellulose 20 (1) (2013) 417–427.
[3] G. Ramorino, F. Bignotti, S. Pandini, T. Riccò, Mechanical reinforcement in natural rubber/organoclay nanocomposites, Compos. Sci. Technol. 69 (7–8) (2009) 1206–1211.
[4] J. Berriot, H. Montes, F. Lequeux, D. Long, P. Sotta, Evidence for the shift of the glass transition near the particles in silica-filled elastomers, Macromolecules 35 (26) (2002) 9756–9762.
[5] K. Hsu-Chiang, M.M. Chen-Chi, C. Wei-Ping, Y. Siu-Ming, W. Hsin-Ho, L. Tzong-Ming, Synthesis, thermal, mechanical and rheological properties of multiwall carbon nanotube/waterborne polyurethane nanocomposite, Compos. Sci. Technol. 65 (11–12) (2005) 1703–1710.
[6] C. Xiaodong, D. Hua, M.L. Chang, New nanocomposite materials reinforced with flax cellulose nanocrystals in waterborne polyurethane, Biomacromolecules 8 (3) (2007) 899–904.
[7] D. Dubief, E. Samain, A. Dufresne, Polysaccharide microcrystals reinforced amorphous poly(β-hydroxyoctanoate) nanocomposite materials, Macromolecules 32 (18) (1999) 5765–5771.
[8] W. Helbert, J.Y. Cavaillé, A. Dufresne, Thermoplastic nanocomposites filled with wheat straw cellulose whiskers. Part I: processing and mechanical behavior, Polym. Compos. 17 (4) (1996) 604–611.
[9] L. Chazeau, J.Y. Cavaillé, G. Canova, R. Dendievel, B. Boutherin, Viscoelastic properties of plasticized PVC reinforced with cellulose whiskers, J. Appl. Polym. Sci. 71 (11) (1999) 1797–1808.
[10] N. Ljungberg, C. Bonini, F. Bortolussi, C. Boisson, L. Heux, J.Y. Cavaillé, New nanocomposite materials reinforced with cellulose whiskers in atactic polypropylene: effect of surface and dispersion characteristics, Biomacromolecules 6 (5) (2005) 2732–2739.
[11] M.R. Ruiz, J.Y. Cavaillé, A. Dufresne, C. Graillat, J.F. Gérard, New waterborne epoxy coatings based on cellulose nanofillers, Macromol. Symp. 169 (1) (2001) 211–222.
[12] M.S. Peresin, Y. Habibi, J.O. Zoppe, J.J. Pawlak, O.J. Rojas, Nanofiber composites of polyvinyl alcohol and cellulose nanocrystals: manufacture and characterization, Biomacromolecules 11 (3) (2010) 674–681.
[13] P. Lu, Y.L. Hsieh, Cellulose nanocrystal-filled poly(acrylic acid) nanocomposite fibrous membranes, Nanotechnology 20 (41) (2009) 1–9.
[14] W. Park, M. Kang, H.S. Kim, H.J. Jin, Electrospinning of poly(ethylene oxide) with bacterial cellulose whiskers, Macromolecular Symposium 249–250 (1) (2007) 289–294.
[15] A. Abdulkhani, J. Hosseinzadeh, A. Ashori, S. Dadashi, Z. Takzare, Preparation and characterization of modified cellulose nanofibers reinforced polylactic acid nanocomposite, Polym. Test. 35 (2014) 73–79.
[16] O.J. Rojas, G.A. Montero, Y. Habibi, Electrospun nanocomposites from polystyrene loaded with cellulose nanowhiskers, J. Appl. Polym. Sci. 113 (2) (2009) 927–935.
[17] H. Liu, D. Liu, F. Yao, Q. Wu, Fabrication and properties of transparent polymethylmethacrylate/cellulose nanocrystals composites, Bioresour. Technol. 101 (14) (2010) 5685–5692.
[18] C. Xiaodong, X. Chuanhui, W. Yanpeng, L. Yu, L. Yuhong, C. Yukun, New nanocomposite materials reinforced with cellulose nanocrystals in nitrile rubber, Polym. Test. 32 (5) (2013) 819–826.

[19] A. Bendahoua, H. Kaddamic, A. Dufresne, Effect of the nano-cellulose content on the properties of reinforced polyurethanes. A study using mechanical tests and positron annihilation spectroscopy, Polym. Test. 32 (1) (2013) 115–122.
[20] E.M. Maafi, F. Malek, L. Tighzert, P. Dony, Synthesis of Polyurethane and characterization of its composites based on alfa cellulose fibers, J. Polym. Environ. 18 (4) (2010) 638–646.
[21] S.J. Eichhorn, A. Dufresne, M. Aranguren, N.E. Marcovich, J.R. Capadona, S.J. Rowan, et al., Review: current international research into cellulose nanofibres and nanocomposites, J. Mater. Sci. 45 (1) (2010) 1–33.
[22] J. Huang, J.W. Zou, P.R. Chang, J.H. Yu, A. Dufresne, New water born polyurethane-based nanocomposites reinforced with low loading levels of chitin whisker, Express Polym. Lett. 5 (4) (2011) 362–375.
[23] L.H.C. Mattoso, E.S. Medeiros, D.A. Baker, J. Avloni, D.F. Wood, W.J. Orts, Electrically conductive nanocomposites made from cellulose nanofibrils and polyaniline, J. Nanosci. Nanotechnol. 8 (5) (2008) 1–6.
[24] K.L. Dagnon, K. Shanmuganathan, C. Weder, S.J. Rowan, Water-triggered modulus changes of cellulose nanofiber nanocomposites with hydrophobic polymer matrices, Macromolecules 45 (11) (2012) 4707–4715.
[25] J.R. Capadona, K. Shanmuganathan, D.J. Tyler, S.J. Rowan, C. Weder, Stimuli-responsive polymer nanocomposites inspired by the sea cucumber dermis, Science 319 (5868) (2008) 1367–1370.
[26] Q. Wu, Y. Meng, K. Conch, S. Wang, Y. Li, L. Ma, S. Fu, Influence of temperature and humidity on nano-mechanical properties of cellulose nanocrystal films made from switchgrass and cotton, Ind. Crop. Prod. 48 (2013) 28–35.
[27] Y. Lu, L. Tighzert, F. Berzina, S. Rondot, Innovative plasticized starch films modified with waterborne polyurethane from renewable resources, Carbohydr. Polym. 61 (2) (2005) 174–182.
[28] M. Floros, L. Hojabri, E. Abrahama, J. Jose, S. Thomas, L. Pothanb, A.L. Leao, et al., Enhancement of thermal stability, strength and extensibility of lipid-based polyurethanes with cellulose-based nanofibers, Polym. Degrad. Stab 97 (10) (2012) 1970–1978.
[29] J. Gao, J. Peng, T. Zhong, J. Sun, X. Wang, C. Yue, Biocompatible elastomer of waterborne polyurethane based on castor oil and polyethylene glycol with cellulose nanocrystals, Carbohydr. Polym. 87 (3) (2012) 2068–2075.
[30] S.H. Park, K.W. Oh, S.H. Kim, Reinforcement effect of cellulose nanowhisker on bio-based polyurethane, Compos. Sci. Technol. 86 (2013) 82–88.
[31] H. Liu, S. Cui, S. Shang, D. Wang, J. Song, Properties of rosin-based waterborne polyurethanes/cellulose nanocrystals composites, Carbohydr. Polym. 96 (2) (2013) 510–515.
[32] Z.S. Petrovic, J. Ferguson, Polyurethane elastomers, Prog. Polym. Sci. 16 (5) (1991) 695–836.
[33] A. Saralegi, M.L. Gonzalez, A. Valea, A. Eceiza, M.A. Corcuera, The role of celulose nanocrystals in the improvement of the shape-memory properties of castor oil-based segmented thermoplastic polyurethanes, Compos. Sci. Technol. 92 (2014) 27–33.
[34] A. Saralegi, L. Rueda, L. Martin, A. Arbelaiz, A. Eceiza, M.A. Corcuera, From elastomeric to rigid polyurethane/celulose nanocrystal bionanocomposites, Compos. Sci. Technol. 88 (2013) 39–47.
[35] M.F. Rosa, E.S. Medeiros, J.A. Malmonge, K.S. Gregorski, D.F. Wood, L.H.C. Mattoso, G. Glenn, W.J. Orts, S.H. Imam, Cellulose nanowhiskers from coconut husk fibers: effect of preparation conditions on their thermal and morphological behavior, Carbohydr. Polym. 81 (1) (2010) 83–92.
[36] M.J. Silva, A.O. Sanches, E.S. Medeiros, L.H.C. Mattoso, C.M. McMahan, J.A. Malmonge, Nanocomposites of natural rubber and polyaniline-modified cellulose nanofibrils, J. Therm. Anal. Calorim. 117 (1) (2014) 387–392.
[37] X.M. Dong, J.F. Revol, D.G. Gray, Effect of microcrystallite preparation conditions on the formation of colloid crystals, Cellulose 5 (1) (1998) 19–32.
[38] S. Neralla, Nanocrystals – Synthesis, Characterization and Applications, Intech, Rijeka, Croatia, 2012.
[39] Y.R. Rhin, D. Zhang, D.H. Fairbrother, K.A. Wepasnick, K.J. Livi, R.J. Bodnar, D.C. Nagle, Changes in electrical and microstructural properties of microcrystalline cellulose as function of carbonization temperature, Carbon 48 (4) (2010) 1012–1024.
[40] G. Chen, M. Wei, J. Chen, J. Huang, A. Dufresne, P.R. Chang, Simultaneous reinforcing and toughening: New nanocomposites of waterborne polyurethane filled with low loading level of starch nanocrystals, Polymer 49 (7) (2008) 1860–1870.